JVST A
Journal of Vacuum Science & Technology A

Optical and mechanical properties of nanolaminates of zirconium and hafnium oxides grown by atomic layer deposition

Cite as: J. Vac. Sci. Technol. A **38**, 022406 (2020); https://doi.org/10.1116/1.5131563
Submitted: 15 October 2019 . Accepted: 27 December 2019 . Published Online: 17 January 2020

Taivo Jõgiaas, Mikk Kull, Helina Seemen, Peeter Ritslaid, Kaupo Kukli, and Aile Tamm

JVST A
Journal of Vacuum Science & Technology A

ARTICLE

avs.scitation.org/journal/jva

Optical and mechanical properties of nanolaminates of zirconium and hafnium oxides grown by atomic layer deposition

Cite as: J. Vac. Sci. Technol. A 38, 022406 (2020); doi: 10.1116/1.5131563
Submitted: 15 October 2019 · Accepted: 27 December 2019 ·
Published Online: 17 January 2020

Taivo Jõgiaas,[1,a)] Mikk Kull,[1] Helina Seemen,[1] Peeter Ritslaid,[1] Kaupo Kukli,[1,2] and Aile Tamm[1]

AFFILIATIONS

[1]Institute of Physics, University of Tartu, W. Ostwaldi 1, 50411 Tartu, Estonia
[2]Department of Chemistry, University of Helsinki, P.O. Box 55, FI-00014 Helsinki, Finland

Note: This paper is part of the 2020 Special Topic Collection on Atomic Layer Deposition (ALD).
[a)]**Author to whom correspondence should be addressed:** taivo.jogiaas@ut.ee

ABSTRACT

Nanolaminates of ZrO_2 and HfO_2 were grown by atomic layer deposition, using metal halides and water as precursors, on silicon and fused quartz substrates at 300 °C. The crystalline phase composition, optical refraction, and mechanical performance of the multilayers were influenced by the relative contents of the constituent metal oxides. The crystal growth in as-deposited HfO_2 dominantly led to the monoclinic phase, whereas ZrO_2 was partially crystallized as its metastable and hard tetragonal polymorph. The hardness and elasticity of the nanolaminate structures could be modified by varying the amounts of either oxide contributing to the crystallographic order formed in the solid films. The refractive indexes depended on the nanolaminate structure.

I. INTRODUCTION

ZrO_2 and HfO_2 are mechanically hard oxides of chemically equivalent metals[1] relevant to a variety of applications, which make these materials scientifically and technologically attractive. Although HfO_2 and ZrO_2 are regarded as structural and chemical analogs, certain differences in their electron structures cause higher ionicity and chemical stability in HfO_2.[2] HfO_2 can be stabilized in the form of its stable monoclinic polymorph more feasibly compared to ZrO_2, whereas the latter can relatively easily be transformed to the tetragonal phase.[3] Therefore, modifications of structure-dependent physical properties, as compared to those of the single metal oxides, can be expected in mixtures or multilayers consisting of HfO_2 and ZrO_2. Such structural modifications may occur tunable and useful while aiming at advanced mechanical or electro-optical properties.

Mixtures and solid solutions of HfO_2 and ZrO_2 have been investigated in several works to date, exemplified by $Hf_{0.5}Zr_{0.5}O_2$ films grown by pulsed laser deposition,[4] $(ZrO_2)_{0.66}(HfO_2)_{0.34}$ films grown by atomic layer deposition (ALD),[5] ZrO_2-HfO_2 stacking layers grown by ALD (Refs. 6 and 7), or ZrO_2-HfO_2 variably mixed films grown either by ALD (Refs. 8 and 9) or by chemical solution deposition.[10]

Nanocomposites, multilayers, or solid solutions based on HfO_2 and ZrO_2, especially in thin film form, have been of interest, namely, due to their electronic,[4,7–10] structural,[6–11] optical,[5] and mechanical[12] properties. We have earlier grown HfO_2-ZrO_2 stacked layers by ALD in order to examine their ability to polarize nonlinearly in external electrical and magnetic fields.[13]

The present study was conducted to investigate the structure and behavior of ZrO_2 and HfO_2 films grown as alternating layers in nanolaminate structures by atomic layer deposition. Refractive indices and mechanical characteristics of ZrO_2-HfO_2 nanolaminates were studied to evaluate the parameters of solid films potentially relevant to microelectromechanical or optical systems, where optically or mechanically adapted coatings are needed.[14,15]

II. EXPERIMENT

All ZrO_2 and HfO_2 thin films were grown via atomic layer deposition using $ZrCl_4$ and $HfCl_4$ precursors at 300 °C in a hot-wall

TABLE I. Film thicknesses, growth rates, and elemental composition of single oxides and nanolaminates.

Cycle scheme	Zr (%)	Hf (%)	O (%)	Cl (%)	(Hf + Zr)/O ratio	Film thickness (nm)	Growth rate (nm/cycle)
$500 \times HfO_2$	—	31.2 ± 0.1	68.4 ± 0.1	0.3 ± 0.1	0.46	64 ± 1	0.13 ± 0.01
$500 \times ZrO_2$	32.5 ± 0.1	—	67.0 ± 0.1	0.5 ± 0.1	0.49	59 ± 1	0.12 ± 0.01
$280 \times (2 \times HfO_2 + 2 \times ZrO_2)$	15.8 ± 0.1	12.2 ± 0.1	71.6 ± 0.1	0.3 ± 0.1	0.39	105 ± 1	0.09 ± 0.01
$70 \times (8 \times HfO_2 + 8 \times ZrO_2)$	17.0 ± 0.1	12.0 ± 0.1	70.6 ± 0.1	0.4 ± 0.1	0.41	109 ± 1	0.10 ± 0.01
$22 \times (25 \times HfO_2 + 25 \times ZrO_2)$	23.5 ± 0.1	6.6 ± 0.1	69.3 ± 0.1	0.5 ± 0.1	0.44	102 ± 1	0.01 ± 0.01

flow-type reactor.[16] All experiments were carried out at a pressure of 2.2 mbar in the growth zone. $ZrCl_4$ and $HfCl_4$ were evaporated from crucibles inside the reactor at 160 ± 2 °C. N_2 was used as carrier and purging gas, and H_2O was used as the oxygen precursor. Cycle times used for the growth of both oxides were 5-2-1-5 s in a given sequence: $ZrCl_4$/$HfCl_4$ pulse-purge-H_2O pulse-purge. Three laminates of ZrO_2 and HfO_2 were deposited on –OH terminated (100)-oriented single-crystal Si and fused quartz substrates. Cycle sequences for the laminates were $280 \times (2 \times HfO_2 + 2 \times ZrO_2)$, $70 \times (8 \times HfO_2 + 8 \times ZrO_2)$, and $22 \times (25 \times HfO_2 + 25 \times ZrO_2)$, 1120, 1120, and 1100 cycles, respectively. For reference samples, 500 cycles of ZrO_2 and HfO_2 were deposited on separate Si (100) substrates.

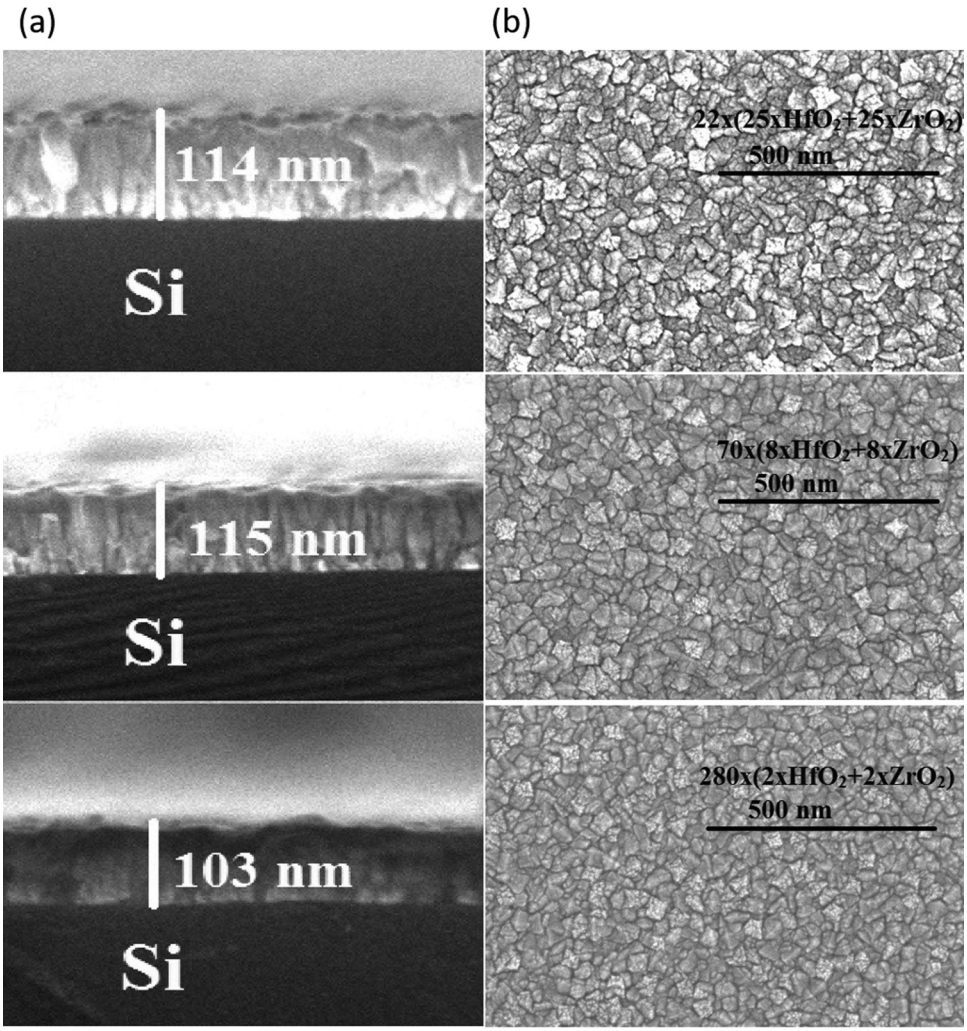

FIG. 1. From top to bottom, cross-section (a) and bird-eye (b) SEM images of nanolaminate films grown using cycle sequences of $22 \times (25 \times HfO_2 + 25 \times ZrO_2)$ (top row), $70 \times (8 \times HfO_2 \times 8 \times ZrO_2)$ (middle row), and $220 \times (2 \times HfO_2 + 2 \times ZrO_2)$ (bottom row).

The SEMILAB GES-5E spectroscopic ellipsometer was used to determine thicknesses, refractive indices, and extinction coefficients of laminates and single oxides on Si (100) substrates. The Cauchy model, which is widely used for dielectric materials, was used for fitting measured and modeled curves in the wavelength range of 257–900 nm.

Laminates and reference samples on Si (100) substrates were further characterized using the wavelength dispersive x-ray fluorescence (XRF) spectrometer Rigaku™ ZSX-400. The LiF (200) analyzing crystal was used for obtaining atomic percentages of Hf and Zr, and Ge (111) and RX40 crystals were used for measuring the contents of Cl and O, respectively.

X-ray diffractometry (XRD) was applied for the determination of the phase composition of laminates and single oxides on Si (100) substrates. All measurements were conducted using the Rigaku™ SmartLab diffractometer with Cu K_α radiation with parallel-beam optics in a 2θ range of 15°–65°. The FEI Helios Nanolab 600 scanning electron microscope (SEM) was used to examine uniformity and surface morphology of the laminates on Si (100) substrates.

Instrumented nanoindentation was used for measuring hardness and elastic modulus of laminates on the fused quartz substrate and the substrate itself. Bruker triboindenter TI 980, equipped with a Berkovich tip, was used in a continuous stiffness measurement mode. The maximum indentation depth and the indentation force were ~300 nm and ~9 mN, respectively, and 15 measurements were averaged before acquiring a single data point. The indenter tip was calibrated on a fused quartz standard with a reduced modulus of 69.6 GPa and a hardness of 9.25 GPa. It is important to note that thin films are usually deposited on some substrates, and, in practical solutions, for instance, in microelectromechanical devices, the thin film and substrate would act together. For this reason, the indenter displacements of up to 300 nm and the related results will be presented as those extending into substrates under films grown to thicknesses not exceeding 50–100 nm. The Oliver–Pharr methodology as an integral part of the analysis software was exploited for the calculation of indentation results.

The triboindenter scanning probe microscopy (SPM) ability was used to investigate the indentation sites. SPM related data analysis was done using GWYDDION 2.53 software.

III. RESULTS

A. Growth rate and stoichiometry

The stoichiometry and impurity content in HfO_2 and ZrO_2 thin films were measured using XRF. All samples contained chlorine (Table I). As water was used as the oxygen source, all thin films could contain hydrogen, which cannot be detected by XRF. Residual chlorine and hydrogen percentages in similar oxide films have been reported in other studies,[17–20] indicating that at 300 °C, there is not enough thermal energy to complete all the surface reaction.[17] All HfO_2 and ZrO_2 thin films had slightly larger oxygen contents than stoichiometric oxides, which may result from adsorbed water, SiO_x interlayer, or residual hydroxyl groups.

Thicknesses and growth rates of all thin films were measured with ellipsometry (Table I). The growth rate of pure ZrO_2 obtained from the reference sample was in a good agreement with values from the literature,[18,19] while HfO_2 had a slightly lower value.[20] As

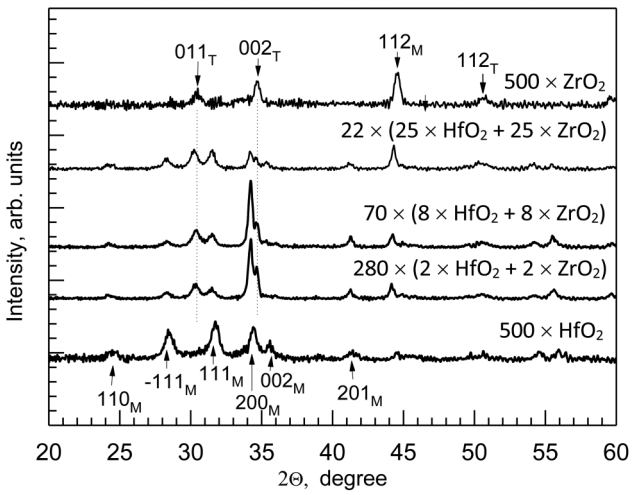

FIG. 2. GIXRD diffractograms for pure ZrO_2, HfO_2, and nanolaminates. The labels at the patterns indicate the cycle schemes of nanolaminates. Miller indices are attributed to corresponding monoclinic (M) and tetragonal (T) phases.

both ZrO_2 and HfO_2 can exist in the monoclinic or tetragonal phase with very similar lattice parameters for both oxides in the same phase, the crystal growth should not be retarded in the case of alternating layers. However, the average growth rates of nanolaminates were smaller than those of single reference oxides, which could be caused by the reduced density of nucleation events while depositing alternating layers of different oxides.[21] It is noteworthy that the content of hafnium in the laminates or mixtures in relation to zirconium, as measured in the present study, remained lower than the nominal content expected after calculating the ratio between

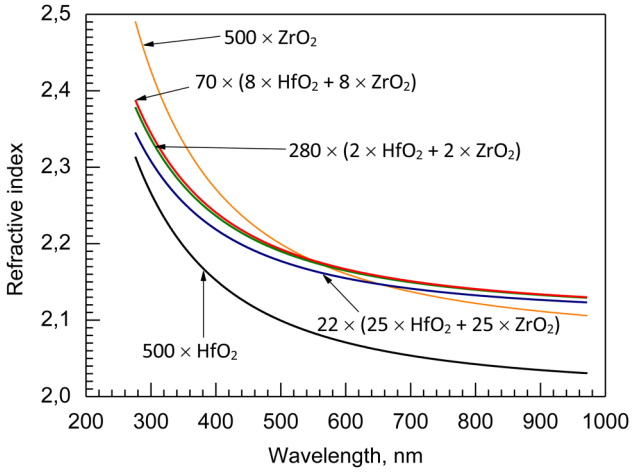

FIG. 3. Refractive index vs wavelength dispersion curves for reference ZrO_2 and HfO_2 reference films as well as nanolaminates. Constituent oxide cycle sequences for the nanolaminates are indicated by labels.

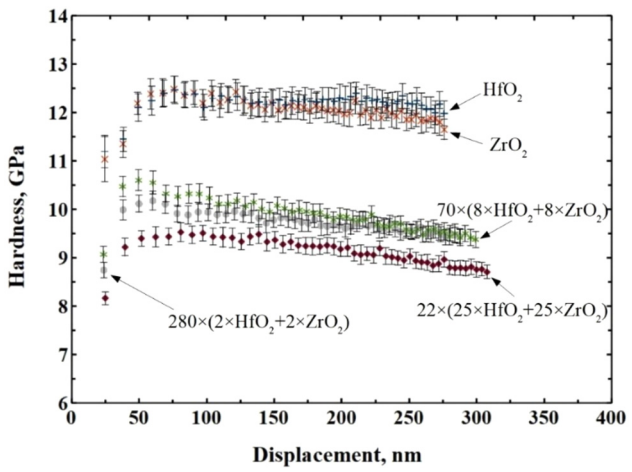

FIG. 4. Hardness against indenter displacement depth for reference ZrO_2 and HfO_2 films and nanolaminates. The growth cycle sequences of the nanolaminate films are given by labels.

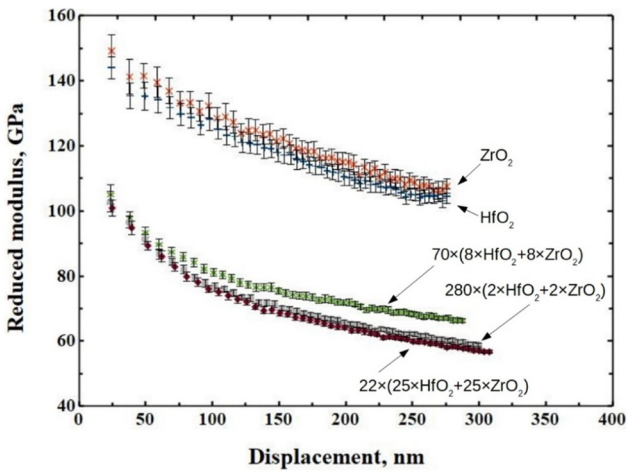

FIG. 5. Averaged elastic moduli of the samples against indenter displacement depth for reference ZrO_2 and HfO_2 films and nanolaminates. The growth cycle sequences of the nanolaminate films are given by labels.

numbers of deposition cycles for HfO_2 and ZrO_2 constituents. Plausibly, HfO_2 has grown with a lower rate on ZrO_2, compared with the growth of ZrO_2 on HfO_2. At this stage, there remains an observation, with reasons behind the phenomenon yet to be clarified.

B. Morphology

Bird-eye and cross-section SEM images of laminates are shown in Fig. 1. Alternating HfO_2 layers with ZrO_2 did not affect the formation and growth of grainy morphology.

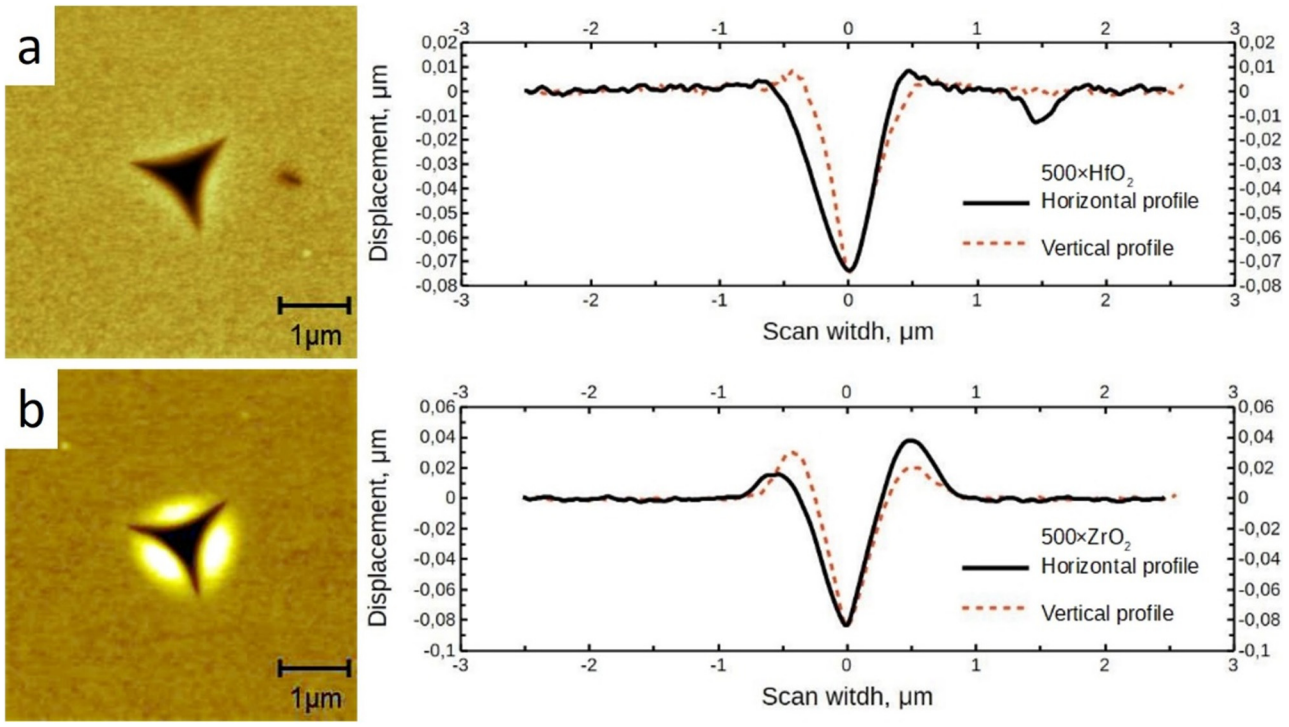

FIG. 6. Scanning probe images of indents of 500 deposition cycles of HfO_2 (a) and ZrO_2 (b), and respective cross-sectional height profiles. Cross-sectional profiles are matched by maximum depth, approximately in the middle of the scanned area.

Figure 2 depicts x-ray diffractograms measured from the films grown in the present study. In the reference ZrO_2 film, the peaks detected in the diffractogram at 30.3°, 34.8°, and 50.4° could be attributed to the 011, 002, and 112 reflections of the tetragonal phase (powder diffraction file (PDF) 00-050-1089) and peaks at 28.2° and 31.4° could be attributed to the monoclinic phase (PDF 00-036-0420) (Fig. 2). In the reference HfO_2 film, the peaks detected in the diffractograms at 24.2°, 28.3°, 31.7°, 34.4°, 35.5°, 41.4°, and 44.8° could be attributed to the monoclinic phase (PDF 00-034-0104) and indexed as 110, −111, 111, 200, 002, 201, 201, and 112, respectively (Fig. 2). In all the nanolaminates deposited on the Si substrate, the −111 and 111 peaks of the monoclinic ZrO_2 (PDF 00-036-0420) and HfO_2 (PDF 00-034-0104) at 28.5 and 31.1°, respectively, and the 011 reflection from the tetragonal phase (PDF 00-050-1089) of ZrO_2 at 30.2° were detected. As one could see, in the nanolaminates where lower numbers of ZrO_2 deposition cycles were used, the contribution from the monoclinic HfO_2 was increased.

Optical dispersion curves from the nanolaminates are depicted in Fig. 3, measured in the wavelength range of 250–970 nm. The nanolaminate grown using the cycle sequence of $22 \times (25 \times HfO_2 + 25 \times ZrO_2)$ with the lowest hardness, as will be described below, also possessed the lowest refractive index of 2.35 at a wavelength of 300 nm. At the same wavelength, the refractive

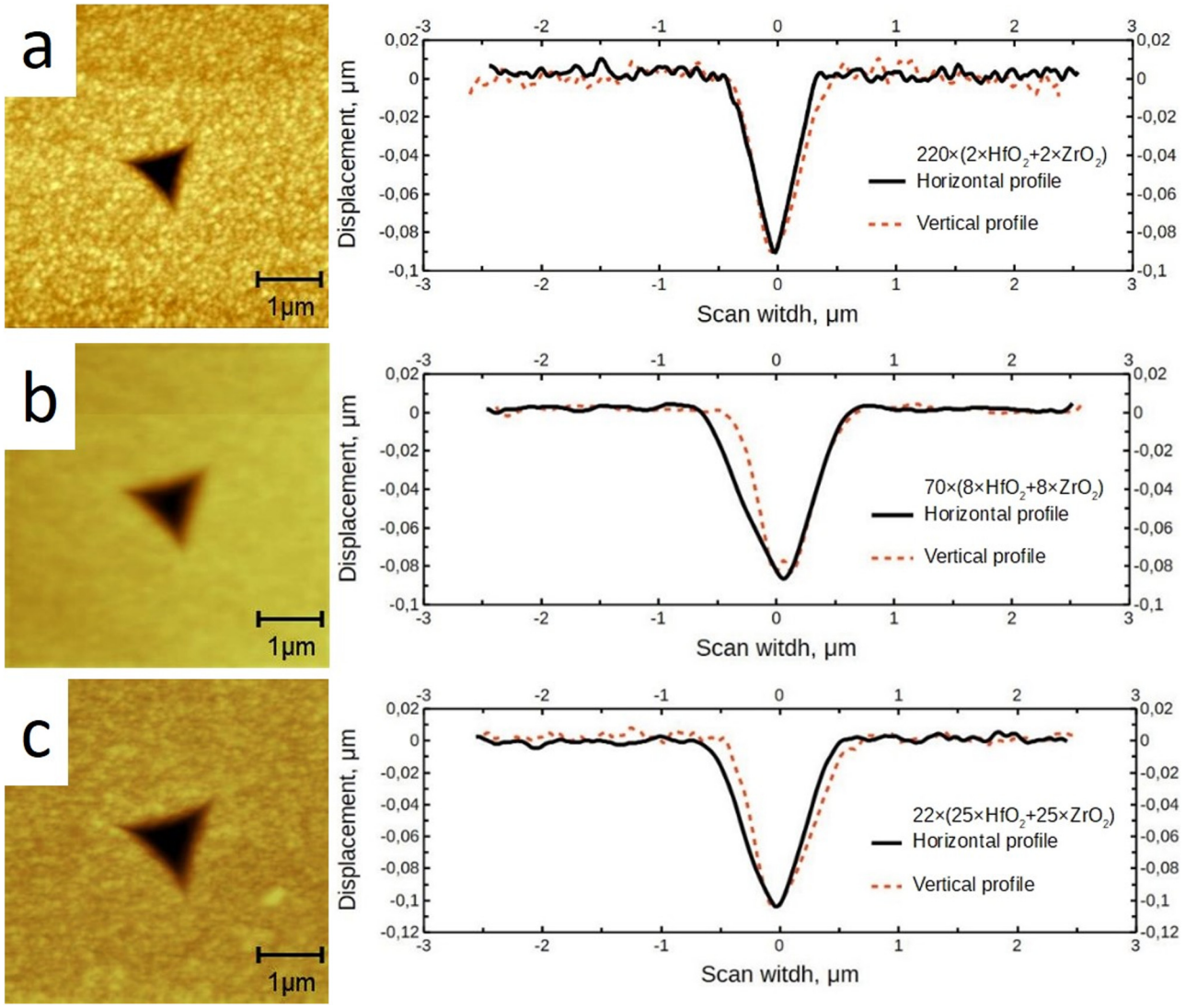

FIG. 7. Indents and respective height profiles in laminates grown using the constituent oxide cycle sequences of $220 \times (2 \times HfO_2 + 2 \times ZrO_2)$ (a), $70 \times (8 \times HfO_2 + 8 \times ZrO_2)$ (b), and $22 \times (25HfO_2 + 25 \times ZrO_2)$ (c) with respective depth profiles.

index for pure ZrO_2 was 2.49, and for pure HfO_2, it was 2.31. As one could actually expect, the refractive index of the nanolaminates generally remained between those of the reference ZrO_2 and HfO_2 films. At higher wavelengths exceeding 560 nm, the nanolaminates possessed higher refractive index values than the reference oxide films, though. This may possibly be due to a large portion of the films crystallized in the high-permittivity form of ZrO_2, i.e., in the form of tetragonal polymorphs. A similar result was measured and reported in previous studies by Aarik *et al.*[20] The absorption coefficient of these films in the wavelength range of 275–970 nm was close to zero, as measured on the Si substrate, which means that the absorption was insignificant. Pervak *et al.*[22] have earlier observed a similar result also in thin films deposited by reactive magnetron sputtering.

C. Hardness and elastic moduli

The hardness and elastic modulus values of the thin films were measured in order to examine possible relations between optical and mechanical properties.

The fused quartz substrate showed similar reduced elastic modulus (Er) and hardness (H) values as the fused quartz calibration sample (about 68 ± 3 GPa and 9 ± 0.5 GPa, respectively). The pure ALD oxides were measured on (100) oriented monocrystalline silicon.

The averaged values of 15 hardness measurements to variable displacement depths with respective standard deviations for every single data point are presented in Fig. 4. The results of the reference oxide measurements indicated that the hardness of both ZrO_2 and HfO_2 films was near 11 GPa. At larger displacements, the data approached the hardness (H = 12 GPa) of the Si(100) substrate[23] as obvious because in such conditions the indentation probes the Si substrate properties.

From the diffraction measurements, one could conclude that HfO_2 was formed mostly in the monoclinic phase, which is not the hardest phase of hafnia or zirconia. The respective values for ALD thin films are 9–14 GPa and about 8 GPa.[15,23,24] In the case of HfO_2, Berdova *et al.*[15] observed that the hardness and elastic modulus were reduced with the content of the hard cubic phase. Further and analogously, for ZrO_2 films, which contained a larger contribution from the harder tetragonal phase,[25] it could be reasonable to expect lower values for laminates with a monoclinic structure.

The average of 15 separate elastic moduli measurements for every single data point with standard deviations is shown in Fig. 5.

The indentation tracks were scanned using a contact mode scanning probe microscope integrated into the indentation system. In silicon, a zirconia thin film was piled up around the indentation mark (Fig. 6). This indicates that the results of ZrO_2 are probably overestimated.

Some pileup could be seen for HfO_2 on the right edge of the dent, but to a lesser extent than for ZrO_2. Pileup was not noticed in the case of laminates (Fig. 7). Material pileup around the tip during indentation could alter the results to overestimate the modulus and hardness value.[26,27]

The depths of the indents in Fig. 7 indicate that the sample grown using the cycle sequence of $22 \times (25 \times HfO_2 + 25 \times ZrO_2)$ are slightly softer compared to other laminates as the plastic deformation depth is somewhat higher. This is in correlation with the results deducted from hardness measurements of the laminates, which reveal about 1 GPa lower hardness for the sample grown using the cycle sequence of $22 \times (25 \times HfO_2 + 25 \times ZrO_2)$.

IV. CONCLUSIONS

Nanolaminates of HfO_2 and ZrO_2 were grown by atomic layer deposition and were grown to the thicknesses of 105 ± 4 nm. In the HfO_2-ZrO_2 nanolaminates, the phase composition could be described as monoclinic and tetragonal polymorphs for ZrO_2 mixed with the monoclinic phase of HfO_2. The absorption coefficient of the films in the wavelength range of 275–970 nm was close to zero, and the refractive index values generally remaining between the values of the reference single metal oxides. At higher wavelengths, the refractive index of nanolaminates tended to exceed those of the constituent oxides measured separately.

The hardest thin films with the highest elastic moduli (11 GPa) were the reference metal oxide films, HfO_2 and ZrO_2, deposited on the Si substrate. The highest hardness (10.6 GPa) was measured for the nanolaminate grown using the ALD cycle sequence of $220 \times (2 \times HfO_2 + 2 \times ZrO_2)$. The lowest hardness (9.5 GPa) was measured for the film grown with the sequence of $22 \times (25 \times HfO_2 + 25 \times ZrO_2)$. The moduli values were around 150 GPa for the reference oxides and 100–110 GPa for the laminates. One can conclude that it is possible to tune the mechanical and optical properties of thin laminates and/or composite HfO_2-ZrO_2 films conveniently upon changing the ratio of the constituent compounds, providing opportunities to adjust coating properties with respect to a substrate.

ACKNOWLEDGMENTS

The research was funded by the European Regional Development Fund (TK134) and Estonian Research Agency (PRG4). This work was partially supported by ERDF project "Center of nanomaterials technologies and research" (NAMUR+, Project No. 2014-2020.4.01.16-0123). The authors are thankful to Dr. Roberts Zabels, the University of Latvia, for technical consultations.

REFERENCES

[1]H. Shin, A. Benali, Y. Luo, E. Crabb, A. Lopez-Bezanilla, L. E. Ratcliff, A. M. Jokisaari, and O. Heinonen, Phys. Rev. Mat. **2**, 075001 (2018).
[2]W. Zheng, K. H. Bowen, J. Li, I. Dąbkowska, and M. Gutowski, J. Phys. Chem. A **109**, 11521 (2005).
[3]M. Forker, P. de la Presa, W. Hoffbauer, S. Schlabach, M. Bruns, and D. V. Szabó, Phys. Rev. B **77**, 054108 (2008).
[4]Y. Wei *et al.*, Nat. Mater. **17**, 1095 (2018).
[5]H. C. Shin *et al.*, J. Surf. Anal. **17**, 203 (2011).
[6]H. Kim, P. C. McIntyre, and K. C. Saraswat, J. Mater. Res. **19**, 643 (2004).
[7]Y. W. Lu, J. Shieh, and F. Y. Tsai, Acta Mater. **115**, 68 (2016).
[8]T. Ali *et al.*, Appl. Phys. Lett. **112**, 22903 (2018).
[9]J. Müller, T. S. Böscke, U. Schröder, S. Mueller, D. Bräuhaus, U. Böttger, L. Frey, and T. Mikolajick, Nano Lett. **12**, 4318 (2012).
[10]S. Nakayama, H. Funakubo, and H. Uchida, Jpn. J. Appl. Phys. **57**, 11UF06 (2018).
[11]D. M. Hausmann and R. G. Gordon, J. Cryst. Growth **249**, 4350 (2003).
[12]M. Boniecki, Z. Librant, and W. Wesołowski, Ceram. Mater. **62**, 259 (2010).
[13]K. Kalam *et al.*, Thin Solid Films **669**, 294 (2019).
[14]E. Cianci *et al.*, Sens. Actutor A **282**, 124 (2018).

[15]M. Berdova, X. Liu, C. Weimer, A. Lamperti, G. Tallarida, E. Cianci, M. Fanciulli, and S. Franssila, J. Vac. Sci. Technol. A **34**, 051510 (2016).
[16]T. Arroval, L. Aarik, R. Rammula, V. Kruusla, and J. Aarik, Thin Solid Films **600**, 119 (2016).
[17]K. Kukli *et al.*, J. Appl. Phys. **96**, 5298 (2004).
[18]K. Kukli, M. Ritala, J. Aarik, T. Uustare, and M. Leskelä, J. Appl. Phys. **92**, 1833 (2002).
[19]J. Aarik, A. Aidla, H. Mändar, T. Uustare, and V. Sammelselg, Thin Solid Films **408**, 97 (2002).
[20]J. Aarik, H. Mändar, M. Kirm, and L. Pung, Thin Solid Films **466**, 41 (2004).
[21]A. Rahtu and M. Ritala, J. Mater. Chem. **12**, 1484 (2002).
[22]V. Pervak, F. Krausz, and A. Apolonski, Thin Solid Films **515**, 7984 (2007).
[23]K. Tapily, J. E. Jakes, D. S. Stone, P. Shrestha, D. Gu, H. Baumgart, and A. A. Elmustafa, J. Electrochem. Soc. **177**, H545 (2008).
[24]T. Jõgiaas *et al.*, Surf. Coat. Tech. **282**, 36 (2015).
[25]T. Jõgiaas, R. Zabels, A. Tarre, and A. Tamm, Mat. Chem. Phys. **240**, 122270 (2020).
[26]A. Bolshakov and G. M. Pharr, J. Mater. Res. **13**, 1049 (1998).
[27]T. Y. Tsui and G. M. Pharr, J. Mater. Res. **14**, 292 (1999).